Elementary Negative Group Delay Filter Functions

Julia Nako[1] · Costas Psychalinos[1] · Brent J. Maundy[2] · Ahmed S. Elwakil[2,3,4]

Abstract

A theoretical study of the behavior of some elementary first- and second-order functions, which are suitable for realizing negative group delay, is performed in this work. As both the gain and phase responses are simultaneously considered, important derivations related to the actual bandwidth of operation are derived accompanied by useful design tips. The presented theory is supported by simulation and experimental results obtained through the utilization of typical active-RC filter structures, as well as from a field-programmable analog array device.

Keywords Negative group delay filters · Analog signal processing · Analog filters · Bilinear filters · Inverse filters · Field-programmable analog array

1 Introduction

Group delay is a measure of the phase response linearity with respect to frequency in systems where the information is carried by the envelope of the signal. Negative group delay (NGD) is observed in filters with a positive slope phase response. Applying a

✉ Costas Psychalinos
  cpsychal@upatras.gr

  Julia Nako
  julia.nako@ac.upatras.gr

  Brent J. Maundy
  bmaundy@ucalgary.ca

  Ahmed S. Elwakil
  elwakil@ieee.org

1 Department of Physics, Electronics Laboratory, University of Patras, 26504 Rio, Patras, Greece

2 Department of Electrical and Software Engineering, University of Calgary, Alberta, Canada

3 Department of Electrical Engineering, University of Sharjah, P.O. Box 27272, Sharjah, United Arab Emirates

4 Nanoelectronics Integrated Systems Center (NISC), Nile University, Giza, Egypt

Birkhäuser

band-limited signal to its input (i.e., the frequency range of the signal is within the bandwidth where a constant group delay is realized), then the filter predictability causes the envelope of the resulting output to advance in time compared to the input signal's envelope [13–16, 28, 29, 32]. This type of filter has been utilized in several interdisciplinary applications, including biomedical signal processing, acoustic signal processing, and chaotic circuits [7, 15, 18, 19, 30].

Negative group delay filter realizations have been already presented in the literature for both base-band and RF band [1, 4, 5, 13, 14, 16, 20–24, 26, 28, 31–33]. In this work, we focus on base-band implementations, particularly those utilizing RC or active-RC circuits [1, 20, 24]. The topologies introduced in [20, 24, 25] are passive RC negative group delay filter designs, which suffer from the absence of cascadability and require additional buffer stages for interconnection. This obstacle has been overcome by the topologies in [12], where first- and second-order NGD filters realized using operational amplifiers (op-amps) as active elements have been presented. The same feature is offered by the topology in [1], where an active-RC second-order filter has been introduced with current feedback operational amplifiers (CFOAs) as active elements. The realized transfer function is an inverse band-pass filter function, which, however, has the limitation of very low gain at low and high frequencies. The second-order topologies introduced in [5] employ also CFOAs as the active elements, and they do not offer a high-impedance input node.

The contribution of this work involves a systematic study of the fundamental negative group delay filter functions by simultaneously considering their gain, phase, and group delay behavior, in order to exploit the practical restrictions. The derivations are accompanied by suitable active-RC implementations evaluated through both simulations and experimental results.

This work is organized as follows: the basic transfer functions of negative group delay filters are presented in Sect. 2, while possible implementations are provided in Sect. 3. The behavior of the considered schemes is evaluated in Sect. 4 through simulation results using the OrCAD PSpice suite and through experimental results using the AN231E04 FPAA platform from Anadigm [2].

2 Negative Group Delay Filters

2.1 First-Order Negative Group Delay Filters

An inverse low-pass filter is described by the transfer function

$$H(s) = G_L(\tau s + 1), \tag{1}$$

with τ being a time constant related to the frequency of the zero (ω_z) of the transfer function, i.e. $\omega_z = 1/\tau$ [11, 16, 28]. This is also equal to the frequency where a 3dB rise of the gain from its low-frequency value is observed and is usually known in the literature as the *knee* frequency ω_k. G_L is the low-frequency gain of the filter. This transfer function has been considered in [11, 16, 28]. The gain and phase responses

of (1) are, respectively, given by:

$$| H(j\omega) | = \sqrt{1 + (\omega\tau)^2}, \tag{2a}$$

$$\angle H(j\omega) = \tan^{-1}(\omega\tau). \tag{2b}$$

Therefore, the group delay of the filter is given by:

$$\tau_g(\omega) \equiv -\frac{\partial}{\partial\omega}\angle H(j\omega) = -\frac{\tau}{1 + (\omega\tau)^2}. \tag{3}$$

According to (3), the group delay is equal to $-\tau$ at low frequencies, while it approaches zero at high frequencies because the bandwidth of the group delay frequency response is determined by the frequency at which $\tau_g(\omega) = 0$, and consequently, it has a theoretically infinite value. It is worth noting that this is an unrealistic consideration because the gain of the filter increases with the frequency and becomes infinite at high frequencies, causing the saturation of the system's output. Therefore, a more realistic definition should be also based on the consideration of the gain of the filter. In particular, assuming that the group delay response is negative within a frequency range of interest, then the "effective" bandwidth is determined by the frequency where a 3dB rise of the gain from its minimum value is observed. For this type of filter, it can be mathematically expressed as:

$$BW_{GD} = \omega_z = \frac{1}{\tau}. \tag{4}$$

A similar problem arises with the gain in the case of the inverse high-pass filter function in (5)

$$H(s) = G_H \frac{\tau s + 1}{\tau s}, \tag{5}$$

where a pole located at zero frequency is added compared to the transfer function in (1). This transfer function has been considered in [23], and since the phase response includes an additional term of $-\pi/2$ compared to (2b), the realized group delay is also described by (3). As the gain of the filter is extremely high at low frequencies (where negative group delay is achieved), it makes this type of filter useless for implementing negative group delay circuits in practice.

Let us now consider the transfer function of a first-order bilinear filter

$$H(s) = G_L \frac{y\tau s + 1}{x\tau s + 1}, \tag{6}$$

with $x, y > 0$ being dimensionless scaling factors and the time constant $\tau = 1/\omega_0$, where ω_0 is a characteristic frequency. The transfer function in (6) can be alternatively written as in (7)

$$H(s) = G_L \left(\frac{\omega_p}{\omega_z} \right) \frac{s + \omega_z}{s + \omega_p}, \tag{7}$$

with the pole (ω_p) and the zero (ω_z) frequencies (located in the left-half of the s-plane) given by

$$\omega_p = \frac{1}{x\tau} = \frac{\omega_0}{x}, \quad \omega_z = \frac{1}{y\tau} = \frac{\omega_0}{y}, \tag{8}$$

both dependent on the values of x and y variables. The magnitude and phase responses of this filter are, respectively, given by (9a)–(9b)

$$| H(j\omega) |= G_L \cdot \sqrt{\frac{1 + (y\omega\tau)^2}{1 + (x\omega\tau)^2}}, \tag{9a}$$

$$\angle H(j\omega) = \tan^{-1}(y\omega\tau) - \tan^{-1}(x\omega\tau), \tag{9b}$$

and the group delay is hence

$$\tau_g(\omega) = -(y - x)\tau \frac{[1 - (\omega\tau)^2 xy]}{[1 + (y\omega\tau)^2][1 + (x\omega\tau)^2]}. \tag{10}$$

Defining as *mean* frequency the geometric mean of the pole and zero frequencies, i.e.,

$$\omega_m \equiv \sqrt{\omega_p \omega_z}, \tag{11}$$

the numerator of (10) becomes zero at $\omega = \omega_m$, and for other frequencies the sign of the numerator changes from positive to negative. For $x < y$ and $\omega < \omega_m$, the group delay is negative and at very low frequencies tends to $-(y - x)\tau$, having a low-pass filter behavior.

Following the previous definition, the bandwidth of the filter is determined taking into account that the gain at high frequencies is expressed by the formula $G_H = G_L (y/x)$ and that at the mean frequency it is equal to the geometric mean of G_L and G_H, i.e.,

$$G_m = \sqrt{G_L G_H} = G_L \sqrt{\frac{y}{x}}. \tag{12}$$

In order for this frequency to be equal to the *knee* frequency, the condition $G_m = \sqrt{2}G_L$ must be fulfilled which consequently means that $y = 2x$, i.e., the restriction $x < y$ is always satisfied. For comparison purposes with the case of the first-order inverse low-pass filter, the following values are chosen: $y = 1$ and $x = 0.5$. Using (11), the resulting expression of the bandwidth is given by: (13) as

$$\text{BW}_\text{GD} = \omega_m = \frac{\sqrt{2}}{\tau}. \tag{13}$$

According to (4) and (13), the realized bandwidth is $\sqrt{2}$ times the corresponding bandwidth of the first-order inverse low-pass filter.

2.2 Second-Order Negative Group Delay Filters

Let us consider the transfer function of an inverse second-order low-pass filter

$$H(s) = G_L \frac{s^2 + \frac{\omega_0}{Q}s + \omega_0^2}{\omega_0^2}. \tag{14}$$

The zeros of (14) are

$$\omega_{z1,2} = -\frac{\omega_0}{2Q}\left(1 \pm \sqrt{1 - 4Q^2}\right), \tag{15}$$

and the gain and phase responses are, respectively,

$$\mid H(j\omega) \mid = G_L \cdot \sqrt{\left[1 - (\omega\tau)^2\right]^2 + \left(\frac{\omega\tau}{Q}\right)^2}, \tag{16a}$$

$$\angle H(j\omega) = \tan^{-1}\frac{\omega\tau}{Q\left[1 - (\omega\tau)^2\right]}. \tag{16b}$$

Therefore, the expression of the group delay is:

$$\tau_g(\omega) = -\frac{\tau}{Q}\frac{1 + (\omega\tau)^2}{\left[1 - (\omega\tau)^2\right]^2 + \left(\frac{\omega\tau}{Q}\right)^2}. \tag{17}$$

According to (17), the filter achieves a negative group delay that approaches $-\tau/Q$ at low frequencies and is dependent on the quality factor of the poles. Assuming a gain response without peaking (i.e., $Q \leq 1/\sqrt{2}$), the (absolute) value achieved is greater than that offered by its first-order counterpart. In terms of bandwidth, in the case of a Butterworth filter function ($Q = 1/\sqrt{2}$), the expression in (4) is still valid.

In the case of second-order inverse high-pass filter described by

$$H(s) = G_H \cdot \frac{s^2 + \frac{\omega_0}{Q}s + \omega_0^2}{s^2}, \tag{18}$$

its behavior in terms of group delay is still described by (17), but faces the same obstacle as its first-order counterpart. The transfer function of a second-order inverse band-pass filter is:

$$H(s) = G_0 \cdot \frac{s^2 + \frac{\omega_0}{Q}s + \omega_0^2}{\frac{\omega_0}{Q}s}, \tag{19}$$
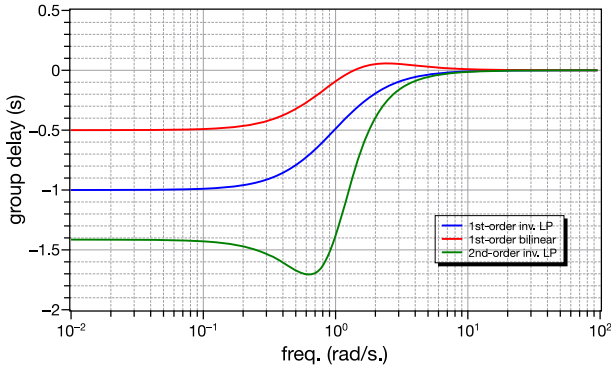
Fig. 1 Group delay responses of the filters described by (1), (6), and (14) ($\omega_0 = 1 rad/s$, $G_L = 1$, $x = 0.5$, $y = 1$ and $Q = 1/\sqrt{2}$)

and its group delay is also described by (17). The problem with this band-pass filter is that the gain exhibits very high values at both low and high frequencies, limiting the circuit's usefulness to a narrow frequency range. It must be mentioned at this point that such systematic comparison of the behavior of the transfer functions in (14), (18), and (19) does not exist in the literature. For further clarity, and considering that $\omega_0 = 1$ rad/s, $G_L = 1$, $x = 0.5$, $y = 1$, and $Q = 1/\sqrt{2}$, the group delay responses of the filters described by (1), (6), and (14) are depicted in Fig. 1.

2.3 Non-Integer-Order Filters

Considering the case of non-integer-order filters, the transfer functions of the fractional-order and power-law inverse low-pass filters are: $H(s) = G_L \left[(\tau s)^\alpha + 1 \right]$ and $H(s) = G_L (\tau s + 1)^\beta$, respectively, with $0 < \alpha, \beta < 1$ being their orders [10]. The corresponding expressions of the realized group delays are:

$$\tau_g(\omega) = -\alpha\tau \frac{\sin(0.5\pi\alpha)}{(\omega\tau)^{1-\alpha} \left[1 + (\omega\tau)^{2\alpha} + 2(\omega\tau)^\alpha \cos(0.5\pi\alpha) \right]}, \tag{20}$$

$$\tau_g(\omega) = -\frac{\beta\tau}{1 + (\omega\tau)^2}, \tag{21}$$

both being negative. According to (20), at low frequencies the group delay is not constant and, also, takes extremely large values; this results from the fact that in this range $t_g(\omega) \sim 1/(\omega\tau)^{1-\alpha}$. Therefore, since it does not offer a constant negative group delay over the range of interest, this transfer function is useless in practice. On the other hand, the group delay realized by a power-law filter is constant at the low-frequency range and its value, resulting from (21) is equal to $-\beta\tau$. This is β times the corresponding group delay realized by a first-order inverse low-pass filter. Taking into account that the *knee* frequency of the filter is given by the formula:

$\omega_k = \omega_z \sqrt{2^{1/\beta} - 1}$, the achieved bandwidth will be:

$$\text{BW}_{\text{GD}} = \omega_k = \frac{1}{\tau} \sqrt{2^{1/\beta} - 1}, \tag{22}$$

which is greater than that realized by its integer-order counterpart, which is given by (4). Assuming, for example, that $\beta = 0.1$, then the bandwidth becomes about 32 times the bandwidth offered by the corresponding integer-order filter.
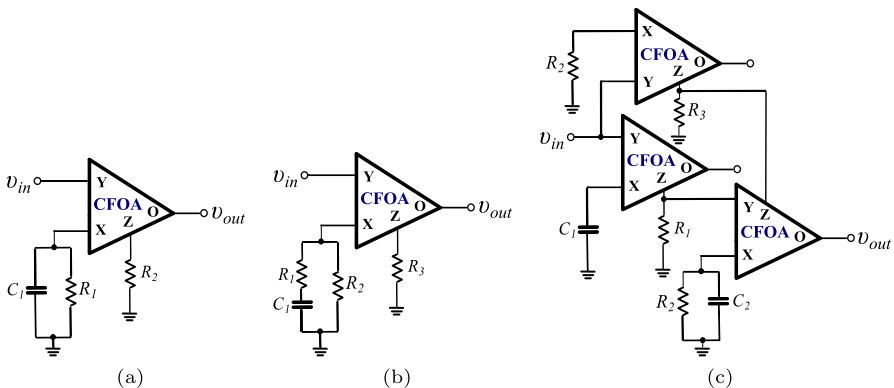
3 Realizations of Negative Group Delay Filter Functions

Employing a CFOA as the active element, the implementation of a first-order inverse low-pass filter is given in Fig. 2a, with the realized transfer function being

$$H(s) = \frac{R_2}{R_1}(R_1 Cs + 1). \tag{23}$$

The implementation of (23) using operational amplifiers as active elements was initially presented in [16] with a low-frequency gain equal to one, but this topology suffers from the presence of a low-impedance input node. By contrast, in the topology of Fig. 2a, the input node offers a high-impedance due to the properties of the CFOA terminals. Comparing (1) with (23), the resulting design equations are: $G_L = R_2/R_1$ and $\tau = R_1 C_1$.

Taking into account the effect of the parasitic resistance (r_X) at the X terminal of the CFOA, the resulting transfer function is

$$H'(s) = H(s) \frac{R_1}{R_1 + r_X} \frac{1}{\tau_X s + 1}, \tag{24}$$

Fig. 2 Realizations of negative group delay using first-order **a** inverse low-pass filter, **b** bilinear filter and **c** second-order inverse low-pass filter

with $H(s)$ being the transfer function which corresponds to the ideal case, and the extra time constant established by the parasitic resistance being

$$\tau_X = \frac{R_1 r_X C_1}{R_1 + r_X} = \tau \frac{r_X}{R_1 + r_X}. \tag{25}$$

The realized group delay function is thus

$$\tau'_g(\omega) = -\tau \frac{R_1}{R_1 + r_X} \frac{1 - (\omega\tau)^2 \frac{r_X}{R_1 + r_X}}{\left[1 + (\omega\tau)^2\right] \cdot \left[1 + (\omega\tau_X)^2\right]}. \tag{26}$$

According to (26), the group delay is negative under the condition

$$\omega < \frac{1}{\tau}\left(1 + \frac{R_1}{r_X}\right). \tag{27}$$

Taking into account that the bandwidth of the group delay in this case is equal to $1/\tau$, it is readily obtained from (27) that the presence of r_X does not affect the realized bandwidth. The value of the group delay at very low frequencies is equal to $R_1/(R_1 + r_X)$; considering a typical value of R_1 equal to $10\,\mathrm{k}\Omega$ and taking into account that the parasitic resistance r_X of the AD844 is equal to $50\,\Omega$, it is obvious that the effect of this resistance is negligible.

Meanwhile, the bilinear filter realization is proposed in Fig. 2b, with the realized transfer function being

$$H(s) = \frac{R_3}{R_2} \cdot \frac{(R_1 + R_2)C_1 s + 1}{R_1 C_1 s + 1}. \tag{28}$$

Assuming that $\tau = (R_1 + R_2)C_1$, then comparing (6) and (28), it is derived that $G_L = R_3/R_2$, $x = R_1/(R_1 + R_2)$, and $y = 1$. The gain at high frequencies is given by the expression: $G_H = 1 + (R_2/R_1)$.

With regards to the effect of the parasitic resistance r_X, the associated transfer function is:

$$H'(s) = \frac{R_3}{R_2 + r_X} \cdot \frac{(R_1 + R_2)C_1 s + 1}{\frac{R_1 R_2 + r_X(R_1 + R_2)}{R_2 + r_X}C_1 s + 1}. \tag{29}$$

Inspecting (28)–(29), it is concluded that the presence of r_X changes the pole of the transfer function from its initial value: $\omega_p = 1/R_1 C_1$ to a value given by (30)

$$\omega'_p = \frac{R_2 + r_X}{R_2 + r_X\left(1 + \frac{R_2}{R_1}\right)} \cdot \omega_p \equiv k \cdot \omega_p. \tag{30}$$

The new location of the pole affects the factor x, which now becomes equal to $x' = kx$ and, consequently, affects the value of the mean frequency (ω_m), and also, the value of

the BW_{GD} by a factor equal to $\sqrt{k}$. At very low frequencies, the group delay will tend to the value $-(y - kx)\tau$. In practice, as the values of R_1 and R_2 are in the order of $k\Omega$ and $r_X = 50\,\Omega$, the parasitic resistance does not cause significant deviation from the theoretically predicted values.

A possible implementation of a second-order inverse low-pass filter is demonstrated in Fig. 2c [8]. Its transfer function is

$$H(s) = \frac{R_3}{R_2} \cdot \frac{s^2 + \frac{1}{R_2 C_2} s + \frac{1}{R_1 R_2 C_1 C_2}}{\frac{1}{R_1 R_2 C_1 C_2}}. \tag{31}$$

Employing (14), the resulting design equations are $G_L = R_3/R_2$, $\omega_0 = (R_1 R_2 C_1 C_2)^{-1/2}$ and $\omega_0/Q = (R_2 C_2)^{-1}$. It is worth mentioning that a passive version of the topology in Fig. 2c is employed in [20]. However, its drawbacks include a $-6\,dB$ gain in the pass band and a maximum possible gain of $0\,dB$.

The transfer function in (6) can be easily realized using the Anadigm AN231E04 FPAA device [2, 9], where the bilinear filter is formed by the summation of a unity gain low-pass filter with pole frequency equal to $\omega_0/2$ and a high-pass filter with the same pole frequency and a maximum gain equal to 2, ensuring that the zero of the realized function will be at ω_0. The clock frequency of the FPAA was set equal to 500 kHz.

## 4 Simulation and Experimental Results

4.1 Simulation Results

Assuming, for example, $\omega_0 = 10\,krad/s$ and $G_L = 1$, the values of the passive elements (rounded to the E96 series defined in IEC 60063 standard) in the case of the inverse filter in Fig. 2a are $R_1 = R_2 = 10\,k\Omega$, and $C_1 = 10\,nF$. The values of passive elements, which are required for implementing the transfer function in (6) by the topology in Fig. 2b with $x = 0.5 = y/2$, $G_L = 1$ and $\omega_0 = 10\,krad/s$, are calculated as $R_1 = R_2 = R_3 = 10\,k\Omega$, and $C_1 = 5\,nF$. Considering the topology in Fig. 2c and assuming that $R_1 = R_2 = 10\,k\Omega$, the other component values for $\omega_0 = 10\,krad/s$ and $Q = 1/\sqrt{2}$ are $R_3 = 10\,k\Omega$, $C_1 = 14\,nF$, and $C_2 = 7.15\,nF$.

Utilizing OrCAD PSpice, with the AD844 CFOA biased at $\pm 10V$ [3], the simulated group delay responses for the filters of Fig. 2a–c are depicted in Fig. 3, with the associated theoretical responses represented by dashed lines. At low frequencies, the group delay values for the inverse first-order filter, the bilinear first-order filter, and the inverse second-order filter are $-99.6\,\mu s$, $-49.8\,\mu s$, and $-139.6\,\mu s$, close to the theoretical ones of $-100\,\mu s$, $-50\,\mu s$, and $-141.42\,\mu s$, respectively. The associated bandwidths are $10.15\,krad/s$, $14.17\,krad/s$ and $10.16\,krad/s$, which are also close to those predicted by the theory, i.e., $10\,krad/s$, $14.14\,krad/s$ and $10\,krad/s$.

Sensitivity analysis is performed by employing the Monte Carlo analysis, offered by the *Advanced Analysis* tool of OrCAD. The statistical plots (for $N = 500$ runs) of the low-frequency group delay and bandwidth of the first-order bilinear filter of
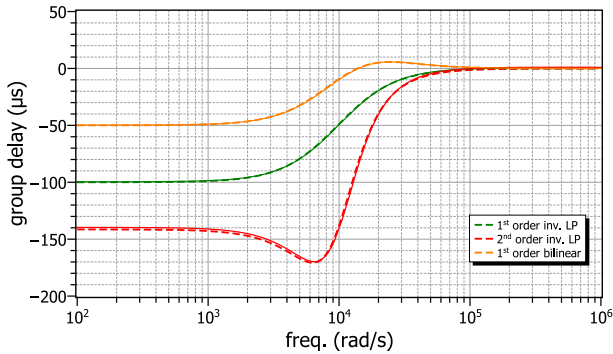
Fig. 3 Simulated responses of the group delays realized by the circuits in Fig. 2a–c
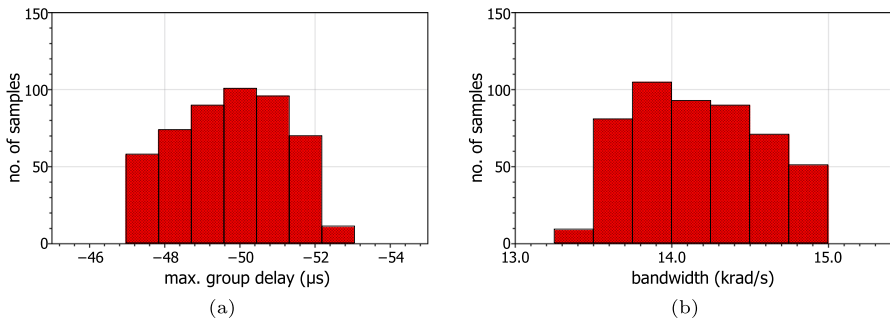

Fig. 4 Monte Carlo analysis results of the low-frequency group delay and bandwidth realized by the topology in Fig. 2b
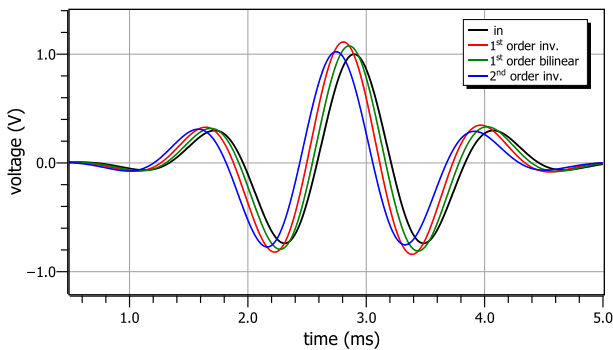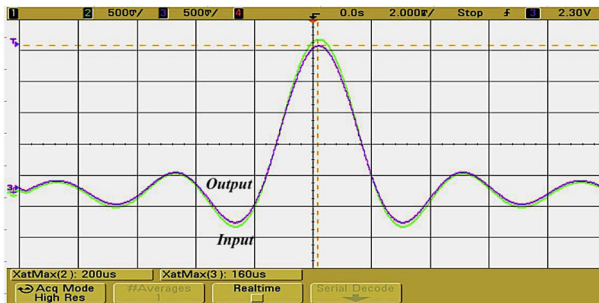

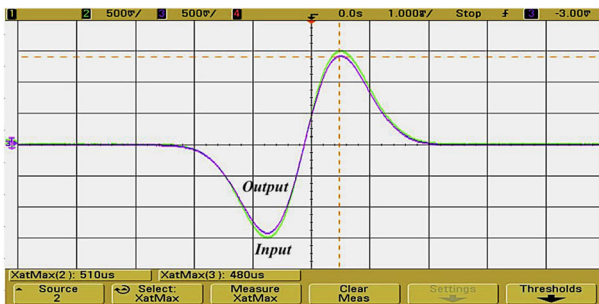**Fig. 5** Time-domain output waveforms of the topologies in Fig. 2a–c stimulated by a Gaussian pulse

Fig. 2b are demonstrated in Fig. 4. The values of the standard deviation are $1.39\,\mu s$ for the group delay and $0.4\,krad/s$ for the bandwidth, which are derived by considering $\pm 5\%$ deviation from the nominal values of passive elements. Given that the mean values are $-49.8\,\mu s$ and $14.17\,krad/s$, this confirms the filter's reasonable sensitivity characteristics.
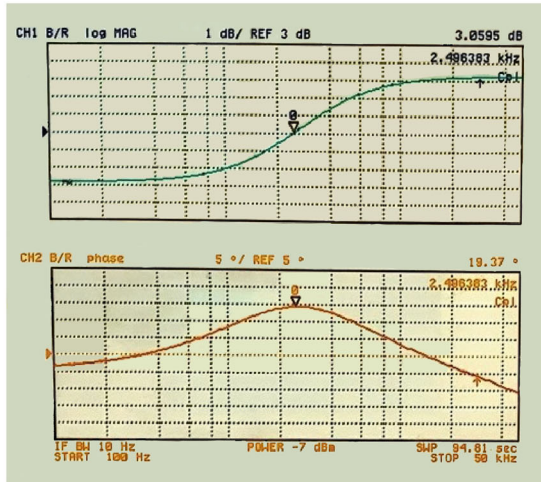
(a)

(b)

(c)

Fig. 6 FPAA experimental results showing **a** the measured magnitude and phase of the transfer function (6) and the observed input and output waveforms on the oscilloscope using **b** a Gaussian mono-pulse input and **c** a Sync input

The time-domain behavior of the topologies under consideration is evaluated using as a stimulus a Gaussian pulse. The resulting output waveforms are depicted in Fig. 5 where the measured delays between the peaks of the envelop of the output signals and the input signal are $-90.2\,\mu$s, $-41.8\,\mu$s, and $-151.3\,\mu$s closely matching the theoretical values of $-89.6\,\mu$s, $-42\,\mu$s and $-164.2\,\mu$s, respectively.

4.2 Experimental Results

The experimental gain and phase frequency responses obtained from the FPAA setup and measured using an HP4395A network/spectrum analyzer are shown in Fig. 6a. The measured bandwidth is 15.63 krad/s, while the theoretical value is 14.17 krad/s. Using the *Keysight IntuiLink Waveform Editor for Arbitrary Waveform Generators®*, a Gaussian mono-pulse input and a Sync input were used as stimulus signals applied through an Agilent 33250A arbitrary waveform generator. The associated screenshots, showing the input and output waveforms on an Agilent DSO 6034A oscilloscope, are depicted in Fig. 6b, c. The measured delays between the peaks of the envelop of the output and input signals were $-30\,\mu$s and $-40\,\mu$s, close to the corresponding theoretical values of $-33.2\,\mu$s and $-43.35\,\mu$s.

5 Conclusion

The study performed in this work demonstrated another important application of inverse filters, complementing those already explored in [17, 27] for realizing a negative group delay. The same holds true for bilinear filters, which have found applications in acoustics as "shelving filters" and in control systems as lead compensators. The suitability of these filters has been approached from a filter design viewpoint where both the gain and phase response were taken into account. Future research steps include the realization of non-integer-order negative group delay filters [6].

Data Availability Data sharing not applicable to this article as no datasets were generated or analyzed during the current study.

Declarations

Conflicts of interest We declare that we do not have any commercial or associative interest that represents a conflict of interest in connection with the work submitted.

References

1. M.T. Abuelmaatti, Z.J. Khalifa, A new CFOA-based negative group delay cascadable circuit. Analog Integr. Circuits Signal Process. **95**, 351–355 (2018). https://doi.org/10.1007/s10470-018-1172-y
2. Anadigm: AN231E04 dpASP: The AN231E04 dpASP Dynamically Reconfigurable Analog Signal Processor. https://www.anadigm.com/an231e04.asp
3. Analog Devices: AD844 60 MHz 2000 V/us Monolithic Op Amp with Quad Low Noise, Data Sheet, Rev. G. https://www.analog.com/en/products/ad844.html. Accessed 5 Sept 2023
4. O. Baloglu, O. Cicekoglu, N. Herencsar, OTA-C signal delay compensation circuit for transimpedance-mode audio signal processing systems. Integration **90**, 205–213 (2023). https://doi.org/10.1016/j.vlsi.2023.02.005
5. O. Baloglu, O. Cicekoglu, N. Herencsar, Single CFOA-based active negative group delay circuits for signal anticipation. Eng. Sci. Technolo. Int. J. **48**, 101590 (2023). https://doi.org/10.1016/j.jestch.2023.101590
6. R. Banchuin, On the fractional domain analysis of negative group delay circuits. Int. J. Circuit Theory Appl. (2024). https://doi.org/10.1002/cta.3819
7. P.Y. Chou, J.F. Chien, K.S. Chen, Y.T. Huang, C.C. Chen, C. Chan, Anticipation and negative group delay in a retina. Phys. Rev. E **103**(2), L020401 (2021). https://doi.org/10.1103/physreve.103.l020401
8. S. Gupta, D. Bhaskar, R. Senani, A. Singh, Inverse active filters employing CFOAs. Electr. Eng. **91**, 23–26 (2009). https://doi.org/10.1007/s00202-009-0112-3
9. A.M. Hassanein, A.H. Madian, A.G. Radwan, L.A. Said, On the design flow of the fractional-order analog filters between FPAA implementation and circuit realization. IEEE Access **11**, 29199–29214 (2023). https://doi.org/10.1109/access.2023.3260093
10. S. Kapoulea, C. Psychalinos, A.S. Elwakil, Power law filters: a new class of fractional-order filters without a fractional-order Laplacian operator. AEU Int. J. Electron. Commun. **129**, 153537 (2021). https://doi.org/10.1016/j.aeue.2020.153537
11. M. Kitano, T. Nakanishi, K. Sugiyama, Negative group delay and superluminal propagation: an electronic circuit approach. IEEE J. Sel. Top. Quantum Electron. **9**(1), 43–51 (2003). https://doi.org/10.1109/jstqe.2002.807979
12. B. Maundy, A. Elwakil, C. Psychalinos, Systematic design of negative group delay circuits. AEU Int. J. Electron. Commun. (2023). https://doi.org/10.1016/j.aeue.2023.155060
13. M.W. Mitchell, R.Y. Chiao, Negative group delay and 'fronts' in a causal system: An experiment with very low frequency bandpass amplifiers. Phys. Lett. A **230**(3–4), 133–138 (1997). https://doi.org/10.1016/s0375-9601(97)00244-2
14. M.W. Mitchell, R.Y. Chiao, Causality and negative group delays in a simple bandpass amplifier. Am. J. Phys. **66**(1), 14–19 (1998). https://doi.org/10.1119/1.18813
15. J. Munday, R. Henderson, Superluminal time advance of a complex audio signal. Appl. Phys. Lett. **85**(3), 503–505 (2004). https://doi.org/10.1063/1.1773926
16. T. Nakanishi, K. Sugiyama, M. Kitano, Demonstration of negative group delays in a simple electronic circuit. Am. J. Phys. **70**(11), 1117–1121 (2002). https://doi.org/10.1119/1.1503378
17. C. Psychalinos, S. Minaei, A. Yesil, First-order inverse filters: implementations using a single voltage conveyor and potential applications. Int. J. Circuit Theory Appl. **50**(10), 3704–3714 (2022). https://doi.org/10.1002/cta.3346
18. T. Pyragiene, K. Pyragas, Anticipatory synchronization via low-dimensional filters. Phys. Lett. A **381**(22), 1893–1898 (2017). https://doi.org/10.1016/j.physleta.2017.04.005
19. T. Pyragiene, K. Pyragas, Design of a negative group delay filter via reservoir computing approach: real-time prediction of chaotic signals. Phys. Lett. A **383**(25), 3088–3094 (2019). https://doi.org/10.1016/j.physleta.2019.07.015
20. R. Randriatsiferana, Y. Gan, F. Wan, W. Rahajandraibe, R. Vauché, N.M. Murad, B. Ravelo, Study and experimentation of a 6-dB attenuation low-pass NGD circuit. Analog Integr. Circuits Signal Process. (2021). https://doi.org/10.1007/s10470-021-01826-x

21. B. Ravelo, Methodology of elementary negative group delay active topologies identification. IET Circuits Devices Syst. **7**(3), 105–113 (2013). https://doi.org/10.1049/iet-cds.2012.0317
22. B. Ravelo, Synthesis of RF circuits with negative time delay by using LNA. Adv. Electromag. **2**(1), 44–54 (2013). https://doi.org/10.7716/aem.v2i1.89
23. B. Ravelo, Similitude between the NGD function and filter gain behaviours. Int. J. Circuit Theory Appl. **42**(10), 1016–1032 (2014). https://doi.org/10.1002/cta.1902
24. B. Ravelo, First-order low-pass negative group delay passive topology. Electron. Lett. **52**(2), 124–126 (2016). https://doi.org/10.1049/el.2015.2856
25. B. Ravelo, H. Bilal, S. Rakotonandrasana, M. Guerin, F. Haddad, S. Ngoho, W. Rahajandraibe, Transient characterization of new low-pass negative group delay RC-network. IEEE Trans. Circuits Syst. II Express Briefs (2023). https://doi.org/10.1109/tcsii.2023.3300124
26. B. Ravelo, A. Pérennec, M. Le Roy, Y.G. Boucher, Active microwave circuit with negative group delay. IEEE Microw. Wirel. Comp. Lett. **17**(12), 861–863 (2007). https://doi.org/10.1109/lmwc.2007.910489
27. R. Senani, D.R. Bhaskar, A. Raj, Inverse analog filters: history, progress and unresolved issues. Electronics **11**(6), 841 (2022). https://doi.org/10.3390/electronics11060841
28. H. Shen, Z. Wang, A circuit principle and simulation test for negative group delay. Int. J. Adv. Netw. Monit. Controls **7**(2), 46–57 (2022). https://doi.org/10.2478/ijanmc-2022-0015
29. D. Solli, R. Chiao, J. Hickmann, Superluminal effects and negative group delays in electronics, and their applications. Phys. Rev. E **66**(5), 056601 (2002). https://doi.org/10.1103/physreve.66.056601
30. H.U. Voss, A delayed-feedback filter with negative group delay. Chaos Interdiscip. J. Nonlinear Sci. (2018). https://doi.org/10.1063/1.5052497
31. F. Wan, L. Wang, Q. Ji, B. Ravelo, Canonical transfer function of band-pass NGD circuit. IET Circuits Devices Syst. **13**(2), 125–130 (2019). https://doi.org/10.1049/iet-cds.2018.5214
32. J.K. Xiao, Q.F. Wang, J.G. Ma, Negative group delay circuits and applications: feedforward amplifiers, phased-array antennas, constant phase shifters, non-foster elements, interconnection equalization, and power dividers. IEEE Microw. Mag. **22**(2), 16–32 (2021). https://doi.org/10.1109/mmm.2020.3035862
33. A. Yuan, S. Fang, Z. Wang, H. Liu, A novel multifunctional negative group delay circuit for realizing band-pass, high-pass and low-pass. Electronics **10**(14), 1742 (2021). https://doi.org/10.3390/electronics10141742